J. Solid St. Sci. & Technol. Letters, 2015, Vol. 16 No. 1-2, pp. 83-87
http://letters.masshp.net/ | ISSN 0128-8393

EFFECT OF PH VARIATION ON MAGNETIC PROPERTIES OF STRONTIUM HEXAFERRITE NANOPARTICLES SYNTHESIZED BY SOL GEL PROCESS

Sakinah Sulaiman[1,], Raba'ah Syahidah Azis[1, 2], Jumiah Hassan[1, 2], Azmi Zakaria[1,2], Nor Nadhirah Che Muda[1], N.M.M.Shahrani[1], Noruzaman Daud[2], Abddul Halim Azizan[2] and Makiyyu Abdullahi Musa[2]*
[1]Instituite of Advanced Technology, Universiti Putra Malaysia, 43400 UPM Serdang,Selangor, Malaysia
[2] Department of Physics, Faculty of Science, Universiti Putra Malaysia, 43400 UPM Serdang,Selangor, Malaysia

ABSTRACT

A strontium ferrite ($SrFe_{12}O_{19}$) nanoparticle was prepared by sol gel auto combustion method at 800 ˚C and 900˚C and at various pH (pH 1, 3 and 5). The $SrFe_{12}O_{19}$ powder was characterized by using Thermogravimetric analyses (TGA), X-Ray Diffraction (XRD), Vibrating Sample Magnetometer (VSM), and Field emission Scanning Microscope (FeSEM) to investigate thermal behavior, crystalline structure, magnetic properties and morphology. To review, the single crystal size of $SrFe_{12}O_{19}$ was found at 900˚C has lower weight loss about 30.44 %, crystalline size of 70.5 nm with M_r, M_s, and H_c were 64036 G, 44.188 emu/g and 27.593 emu/g. The average grain size was 80 ~ 100 nm. In brief, as pH increase, the M_r, M_s and H_c were increases.

Strontium ferrites, well known as hard ferrite, are important ferromagnetic oxides that produce an excellent corrosion resistance, good thermal durability, and high chemical stability, unique electric and magnetic properties. The M-type strontium hexaferrites $SrFe_{12}O_{19}$ (SrM) have been considered by its high density media due to its excellent chemical stability, large magnetocrystalline anisotropy, high intrinsic coercive force and high resistivity [1-4]. Hard ferrites widely use in a permanent magnet motor, loudspeakers, telecommunication, magneto optical, high density magnetic recording devices, and microwave device [5]. Apart from applications in permanent magnets, nanostructure strontium ferrite powders with narrow particle size distribution are suitable for perpendicular high density recording media because they are desirable to increase the capacity of information storage [6-7]. The physical properties of SrM microstructure are fundamentally related to the morphology, crystal structure and size, which can vary depending on the preparation route. There are several methods used to synthesize strontium hexaferrite such as metallorganic chemical vapor deposition, sputtering, pulsed laser deposition, co-precipitation, hydrothermal and sol–gel. The sol– gel route has received considerable attention in the last few years. Some efforts have been carried out to modify the sol–gel process parameters such as pH, basic agent, carboxylic acid, and starting metal salts for further decreasing of the calcination temperature and achieving the finer crystallite size [8]. Masoudpanah & Ebrahimi [9] state that the prefer molar ratio of Fe/Sr is 10 with calcination temperature on the formation of SrM show a single phase at relatively low temperature, i.e. 800 ^{o}C . In addition, XRD showed that the crystallite sizes at range of 20-50 nm. The magnetic properties of this preferred molar ratio exhibit a good saturation magnetization (267 emu/cm^3), high coercivity (4290 Oe) and a relatively high remanent magnetization (134 emu/cm^3). Minh *et al.* [10] state that prefer molar ratio is at 11. The obtain $SrFe_{12}O_{19}$ have high purity, ultrafine size and high coercivity at H_c= n6315 Oe. In this paper, the $SrFe_{12}O_{19}$ nanoparticles will be prepared by using sol-gel citrate nitrate auto combustion process with varied pH control (pH 1, 3 and 5). The effect of pH on the thermal, structural and magnetic properties of $SrFe_{12}O_{19}$ will be discussed.

Strontium ferrite nanoparticles were prepared via sol gel method. High purity of Strontium anhydrous granular $Sr(NO_3)_2$, (Alfa Aesar, 98 %), Iron (III) ferrite $Fe(NO_3)_3$, (HmbG, 99 %), Citric acid $C_6H_8O_7$ (Alfa Aesar, 99 %) was weighted accurately according to stoichiometry equation with the ratio of citrate to nitrate is 0.75. The metal salt solution was mixed in deionized water and heats up on the hot plate at 80 ˚C and stirred at 250 rpm to dissolve the metal salt mixture. The aqueous ammonia NH_3 was added to increase the pH value of the mixture. When the solution is formed, citric acid was added as chelating agent. The hot plate is then increased 100 ˚C, and it slowly turns the solution become a dark brown gel. The gel was then burnt at 200 ˚C to form a black powder. The powder of different pH then heated at 800/900˚C for 6 hour at heating rate of 5˚C/min. The $SrFe_{12}O_{19}$ powders were characterized by using Thermogravimetric analyses (TGA), X-Ray Diffraction (XRD), Vibrating Sample Magnetometer (VSM), and Field emission Scanning Microscope (Fe-SEM).The thermal behavior were obtained using TGA/SDA851˚ Mettler Toledo at temperature range 0 ˚C - 1000˚C with heating rate 5˚C /min . Meanwhile, the crystalline structural characterization of XRD was performed using a Philips Diffractometer Model 7602 EA

Almelo with Cu Kα radiation operated at 4.0 kV and 35 mA. The VSM were measured the properties of magnetic material that obtained from LakeShore. The surface morphology was observed using a FEI Nova NanoSEM 230 scanning electron microscope. Microstructural measurements such as average grain size, as well as their distributions were obtained using these images. The distributions of grain sizes were obtained by taking at least 100 different grain images for the sample and estimating the mean diameters of individual grains by using the J-image software.

The TGA was performed using 8.3609 mg of $SrFe_{12}O_{19}$ sinter at 800˚C and 900˚C. Figure 1 shows the changes in weight with relation to the changes in temperature. The $SrFe_{12}O_{19}$ powder heated at 900˚C has weight loss about 30.44 % and powder heated at 800˚C has weight loss at 35.09 %. From the TGA curve, there are three exothermic peaks shown at approximately 140˚C, range 380˚C - 400˚C and range 690˚C - 700˚C due to decomposition process. The first two exothermic peaks were tending to the decomposition of NH_4NO_3 that liberate NO, O_2, and H_2O [11]. Meanwhile at stage 690˚C -700˚C shows that the decomposition of citric acid and the breakdown of the Fe_2O_3 to Fe as reported by Beretka and Brown [12].

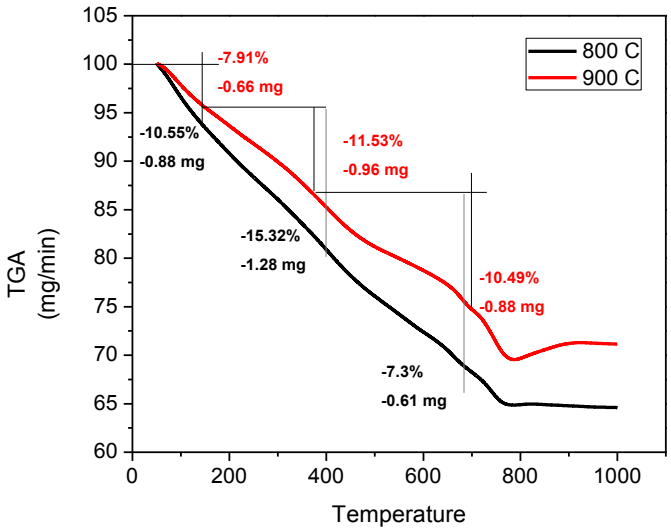

Figure 1: Weight loss versus temperature for $SrFe_{12}O_{19}$ powder of sol gel synthesis at 800 ˚C and 900˚C

Figure 2 shows the XRD spectra of sol gel powder. The XRD peaks are compare to the standard ICSD strontium dodecaferrite, $SrFe_{12}O_{19}$ JCPDS no. 33-1[13]. As powder heated at 800 ˚C, the presence of small amounts of hematite Fe_2O_3 were shown at 2θ peak position, 35.6509 (Figure 2(a)). The single phase $SrFe_{12}O_{19}$ is completely formed with increase the heating temperature to 900 ˚C. Figure 2(b) shows the XRD spectra for $SrFe_{12}O_{19}$ powder, prepared with ammonia added at different pH values. As the pH increases, the intensity counts for powders pH 1 to 3 is increases. However, the intensity decreases from pH 3 to 5 as pH increase. With increasing the heating temperature to 900^{o}C, the line width of the diffraction line decreases and increases, respectively, shows the improvement of the crystallinity and the increase in grain size. The crystallite size for powder heated at 800˚C is 56 nm and 85 nm at 900˚C. However, as the pH increase, the crystalline size is decreases. The average crystallite size of samples obtained is tabulated in Table 1. The average crystallite size determined from the full width at the half maximum (FWHM) of the XRD patterns, using the Scherer formula:

$$D = 0.94\lambda / B_{1/2} \cos\theta \quad (1)$$

where D is the diameter of the crystallite ; λ is the x-ray wavelength; $B_{1/2}$ is the line broadening obtained from $B_{1/2} = (B_2 - b_2)^{0.5}$ where B is the FWHM (full width at half maximum) of the broadened diffraction line on the 2θ scale (radians) and b is the FWHM of a reference sample with large, well-ordered crystallites [14].

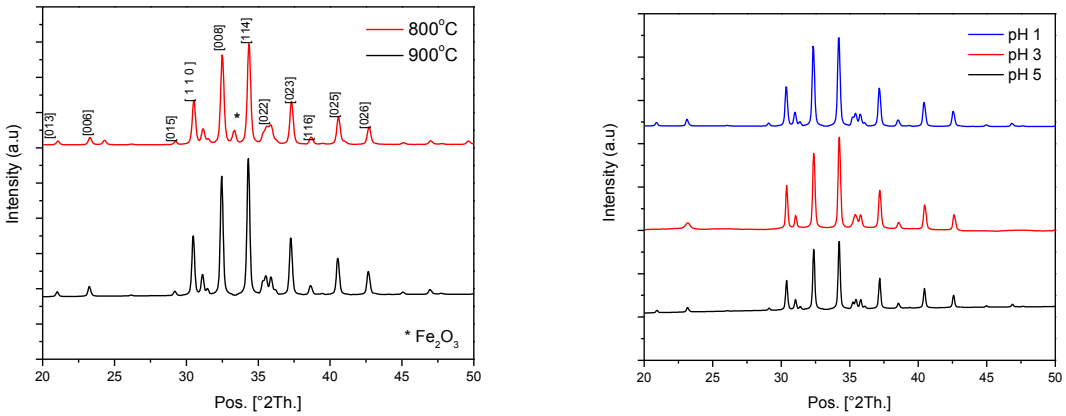

(a) (b)

Figure 2: X-Ray Diffraction of $SrFe_{12}O_{19}$ (a) heated at 800/900°C, (b) $SrFe_{12}O_{19}$ with ammonia with different pH at 900˚C

Table 1: The parameter of pH, 2θ, FWHM, crystallite size and magnetic properties of $SrFe_{12}O_{19}$ powder.

Temp. (˚C)	pH	Pos.[˚2θ]	FWHM	Estimation of crystalline size (nm)	Ms (emu/g)	Mr (emu/g)	H_c (G)
800	-	34.3665	0.1624	57.3	7.144	4.417	6200.1
900	-	34.3150	0.4890	85.7	44.188	27.593	6403.6
	1	34.2024	0.1299	140.9	4.776	2.998	6094.7
	3	34.2154	0.1624	91.3	2.168	1.362	5966.1
	5	34.2303	0.1663	87.5	2.016	1.302	6007.5

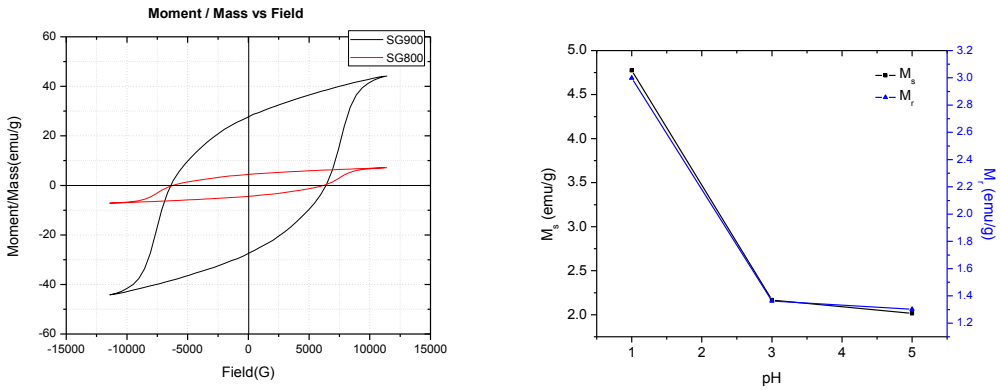

(a) (b)

Figure 3: (a) The magnetic hysteresis loop of $SrFe_{12}O_{19}$ sample at 800˚C and 900˚C, (b) Relation of pH on saturation magnetization M_s remnant M_r of samples.

Figure 3 shows the magnetic hysteresis loop for samples heated at 800/900°C. Powder heated at 800˚C, has relatively low saturation magnetization M_s, remanent magnetization M_r and coercivity H_c of 7.144 emu/g, 4.417 emu/g and 6200.1 G, respectively. Conversely, 900°C powder has high Ms, Mr and H_c reported as shown in Table 1. According to Ju and Rong [15], the coercivity decreases due to the presence of 10 % of α-Fe_2O_3 at 800˚C as shown in Figure 2(a). From Table 1, indicates the effect of pH on magnetic properties of M_s, M_r, and H_c. The magnetic properties of M_s, M_r, and H_c decreases as a function of pH. Nga *et. Al* [15] also confirmed the H_c basically decrease with increasing pH, disputes the slightly change in M_s. Samples at pH 1 exhibit better magnetic properties with H_c of 60.94 G, M_s of 4.767 emu/g and M_r of 2.998 emu/g compare with others pH 3 and pH 5. While, at pH 3 the M_s of 2.168 emu/g, M_r of 1.3619 emu/g and H_c of 5996.1 emu/g. For sample ph 5, the M_s give a value of 2.0156 emu/g, M_r of 1.3020 emu/g and H_c of 6007.4 G. The maximum value of coercivity was 6404 G for the sample at 900 °C (without ammonia). Figure 4 shows FeSEM images of $SrFe_{12}O_{19}$ samples without ammonia (Figure 4(a)) and pH 3 (Figure 4(b)) heated at 900˚C. The average grain size are about 500 nm to 800 nm, respectively. The average grain size of each bulk of $SrFe_{12}O_{19}$ nanoparticles sample is 80 ~ 90 nm. Nga *et al.* [15] highlights that the critical single domain of SrM hexagonal ferrite is 270 nm.

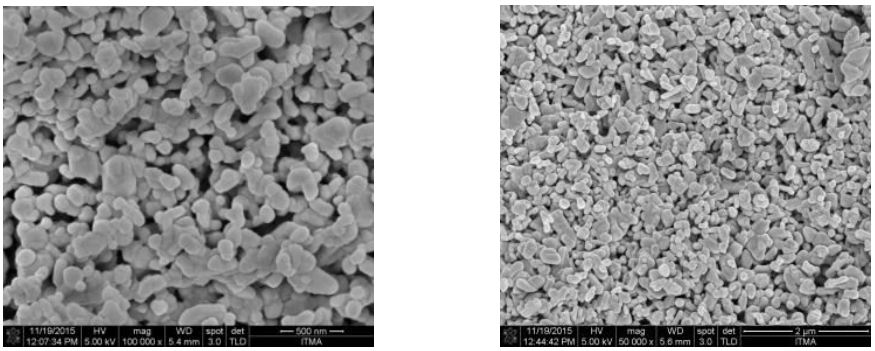

(a) (b)

Figure 4: FeSEM micrographs of the $SrFe_{12}O_{19}$ samples without pH at different sintering temperature at 900˚C (a) without ammonia (b) with ammonia, pH 3

The $SrFe_{12}O_{19}$ nanoparticles were synthesized successfully by sol-gel auto-combustion method. The effect of variation of pH on magnetic properties of $SrFe_{12}O_{19}$ also studied. Investigated the effect of heating temperature and pH value on thermal behavior, crystalline structure, magnetic properties and morphology of $SrFe_{12}O_{19}$ nanoparticles are also observed. The results shows that increase heating temperature to 900°C, leading to an increase in coercivity H_c, saturation magnetization M_s and remnant M_r. A maximum coercivity value of 64004 G and a saturation magnetization value of 44.2 emu/g were obtained for the sample calcined at 900 °C. Variation in pH and ammonia added in $SrFe_{12}O_{19}$ gives decrease the coercivity and saturation magnetization. These hexagonal Sr-ferrites are interesting in applications such as permanent magnets and high-density magnetic recording media.

REFERENCES

[1] S. Sugimoto, S. Kondo, K. Okayama, H. Nakamura, D.Book, T. Kagotani, M. Homma, H.Ota, M. Kimura, (1999). R.Sat, *IEEE Trans. Magn.* 35, 3154-3156.

[2] V.G. Harris, Z. Chen, Y. Chen, S.Yoon, T. Sakai, A. Gieler, A. Yang, Y. He, (2006). *J. App. Phy.* 99, 206-214.

[3] J.L. Went, G.W. Ratenau, E.W. Gorter, G.W. van Oosterhout, Ferroxdure,(1952). *Philips Techn. Rev.* 13, 194-208.

[4] X. Sui, M. Scherge, M.H. Kryder, J.E. Snyder, V.G. Harris, N.C. Koon, (1996). *J. Magn. Magn. Mater.* 155, 132-139

[5] Kanagesan, S., Jesurani, S., Velmurugan, R., & Kalaivani, T. (2012). *J. Mater. Sci. Mater Elec.,* 23(4), 952-955

[6] T. Fujiwara, (1985). IEEE Transactions 21, 1480–1485.

[7] K. Yamamori, T. Suzuki, T.M. Fujiwara, (1986). *IEEE Trans.* 22, 1188–1190.

[8] Masoudpanah, S. M., Ebrahimi, S. A. S., & Ong, C. K. (2012). *J. Magn. Magn. Mater. 324*(18), 2894–2898.

[9] Minh, T., Dang, H., Trinh, V. D., & Bui, D. H. (2012). *Adv. Nat. Sci.: Nanosci. Nanotechnol. 3*, 025015-21

[10] Masoudpanah, S. M., & Ebrahimi, S. A. S. (2012). *J. Magn. Magn. Mater.*, *324*(14), 2239–2244. doi:10.1016/j.jmmm.2012.02.109

[11] Masoudpanah, S.M., & Seyyed Ebrahimi, S. a. (2011). *J. Magn. Magn. Mater.*, 323(21), 2643-2647.

[12] Choy, Y., Wang, J., & Bee, G. (2014). *Proc.Engin.,* 76, 45–52.

[13] Beretka, J., Brown, T., 1971, *Aust. J. Chem.* 24, p. 237.

[14] Ikhwan M. K. 1, Azis R.S., Hashim M., Holland D., Howes A.P., Zakaria A. and Hassan J., (2014). *J. Aust. Ceram. Soc*., 50(2), 17 – 24

[15] Cong-ju, L. & Guo-rong, X., (2011). *Mater. Res. Bull.*, *46*(1), 119–123.